Stability Analysis of Deformation-Monitoring Network Points Using Simultaneous Observation Adjustment of Two Epochs

A. R. Amiri-Simkooei, M.ASCE[1]; S. M. Alaei-Tabatabaei[2]; F. Zangeneh-Nejad[3]; and B. Voosoghi[4]

Abstract: An important issue in deformation analysis is identification of (un)stable points in a monitoring network. This paper proposes a new method that identifies the unstable points of a network based on the generalized likelihood ratio (GLR) test. The method, which simultaneously uses the observations of two epochs, is called the simultaneous adjustment of two epochs (SATE) method. The existing methods apply individual least-squares adjustment to the observations of each epoch. SATE is applicable to one-, two-, or three-dimensional deformation networks with any type of observations, including distances, angles, global positioning system (GPS) baselines, and height difference. To investigate the performance of the proposed method, observations of a real GPS deformation-monitoring network were used. The results for unstable points identification are identical to those of the existing methods. Furthermore, a few simulation case studies were used to evaluate the efficacy of the proposed method. The simulated results for the deformation-monitoring networks, with different scenarios, confirm that the proposed method always performs the best. This method can thus be introduced as a reliable method that provides results that are superior to those of the two existing classical methods. **DOI: 10.1061/(ASCE)SU.1943-5428.0000195.** © *2016 American Society of Civil Engineers.*

Author keywords: Displacement networks; Point stability; Simultaneous adjustment; L1 norm; Global congruency test; Iterative weighted similarity transformation (IWST).

Introduction

Deformation networks have a wide range of applications in the monitoring of engineering constructions, landslide regions, tectonic fault lines, and crustal deformation (Setan and Sing 2001; Hekimoglu et al. 2002, 2010; Erdogan and Hekimoglu 2014). There are different methodologies and techniques for monitoring the deformation. The measurement techniques can be categorized into two main groups: (1) geodetic methods, and (2) geotechnical/structural methods (Setan and Sing 2001; Setan et al. 2003). Each of these measuring methods has its own applications.

The geotechnical/structural methods use instruments such as accelerometers, extensometers, inclinometers, magnetic columns, piezometers, tiltmeters, vibration meters, and strainmeter to measure changes in length, inclination, relative height, and strain. These geotechnical instruments are usually embedded in the studied object during the monitoring project. They give only localized information on the deformation behavior of the object under investigation. More detailed information on these methods are provided by, for example, Forward (2002) and Rüeger (2006).

Geodetic methods can provide some global information on absolute and relative displacements (the distortion of the configuration of the body) of the object under study. Deformation can be obtained through a network of points using repeated geodetic measurements at two or more epochs of time. Geodetic methods are further classified into two main types of monitoring networks: the reference (absolute) networks and relative networks (Chrzanowski et al. 1986).

In an absolute network, some of the points/stations are located outside the deformable part of the body or object being monitored. Using these reference points, the absolute displacements of the monitoring object can be obtained. However, in a relative network, all of the surveyed points are assumed to be located on the deformable body without a set of reference points. In this case, only the relative movements or the distortion of the configuration of the body can be obtained. This paper focuses on the geodetic method using a reference network to monitor the deformation.

For deformation analysis in absolute networks, a control deformation network is to be designed and established. This network consists of a few reference and a few object points in the survey area. The precise position of the network points has to be measured in a few epochs by the techniques of terrestrial surveying, space techniques, or a combination of both. In these networks, the coordinate system or the datum of the network is to be defined over the reference points, hence it needs to be stable (fixed) during the time span of the measurement epochs. Otherwise, the estimated deformation of the network's points could partly be due to the change in the network datum. The estimated deformation is then distorted if a reference point remains fixed in the least-squares (LS) adjustment procedure, whereas in reality, it has moved between the observation

[1]Associate Professor, Dept. of Geomatics Engineering, Faculty of Engineering, Univ. of Isfahan, Hezar-Jarib Ave., 8174673441 Isfahan, Iran. E-mail: amiri@eng.ui.ac.ir

[2]Postgraduate Master, Dept. of Geodesy, Faculty of Geodesy and Geomatics Engineering, K. N. Toosi Univ. of Technology, Mirdamad Ave., 19697-64499 Tehran, Iran (corresponding author). E-mail: sm.alaei@gmail.com

[3]Lecturer, Dept. of Geomatics Engineering, Faculty of Engineering, Univ. of Isfahan, Hezar-Jarib Ave., 8174673441 Isfahan, Iran; Ph.D. Student, Dept. of Surveying and Geomatics Engineering, Geodesy Division, Faculty of Engineering, Univ. of Tehran, North-Kargar Ave., Amir-Abad 14395-515, Tehran, Iran. E-mail: farzanehzangeneh@yahoo.com

[4]Associate Professor, Faculty of Geodesy and Geomatics Engineering, K. N. Toosi Univ. of Technology, 19697-64499 Tehran, Iran. E-mail: vosoghi@kntu.ac.ir

Note. This manuscript was submitted on August 20, 2014; approved on April 5, 2016; published online on May 17, 2016. Discussion period open until October 17, 2016; separate discussions must be submitted for individual papers. This paper is part of the ***Journal of Surveying Engineering***, © ASCE, ISSN 0733-9453.

campaigns. The stability analysis of the reference points is thus an important issue in deformation analysis. This issue has been extensively investigated by many researchers over the past decades. Among the researchers who have been engaged in studies on point-stability analysis and deformation monitoring, one may at least refer to the studies by van Mierlo (1978), Niemeier (1979), Fraser and Gruendig (1984), Cooper (1987), Chen (1983), Chen et al. (1990), Setan (1995), Caspary (1987), Setan and Sing (2001), Hekimoglu et al. (2002. 2010), Hekimoglu and Erdogan (2012), Erdogan and Hekimoglu (2014), Denli (2008), Taşçi (2010), and Aydin (2011).

Different methods of stability analysis and deformation monitoring are based on the LS estimation, and are referred to as the conventional deformation analyses (CDA) (Niemeier 1985; Chen 1983; Hekimoglu et al. 2010; Erdogan and Hekimoglu 2014). The CDA suffers from unrecognized nonrandom disturbances, such as blunders or outliers, that may erroneously affect the results. Therefore, the CDA still needs to be developed/improved to overcome such problems. Hekimoglu et al. (2002, 2010) and Hekimoglu and Erdogan (2012) investigated the reliability of the CDA methods using the concept of mean success rate proposed by Hekimoglu and Koch (1999, 2000) for outlier test methods. They showed that the most reliable results are always obtained if there exists only one displaced point. They thus proposed a strategy that works on an absolute deformation-monitoring network based on the division of the whole network into subnetworks. Each subnetwork consists of only one object point, and other points are assumed to be stable. Hekimoglu et al. (2010) and Hekimoglu and Erdogan (2012) showed that such a design improves the reliability of the CDA. In this case, the mean success rate of the subnetworks is larger than that of the whole network.

Deformation analysis methods can generally be classified into two categories: robust methods and nonrobust methods (Nowel and Kamiński 2014). The classical robust methods are based on the results of the separate LS adjustments of two epochs. They use the Helmert similarity transformation (see Baarda 1981; Teunissen 1985) of the differences in the adjusted coordinates of the two epochs with the optimization principle of robust estimation. The obtained displacement vectors of single points are then evaluated for their statistical significance. The distinct robust methods differ in the optimization condition used. For example, the iterative weighted similarity transformation (IWST) is one of the well-known robust methods that minimizes the L1 norm of the displacement vector (Chen 1983; Chen et al. 1990). The nonrobust methods are also based on the results of the separate LS adjustments of two epochs, which are formulated using statistical testing. Global congruency testing is the most popular method in this group (van Mierlo 1978; Niemeier 1979; Fraser and Gruendig 1984; Cooper 1987).

There are also many other new methods, which are based on the robust estimation principle. One may at least refer to the *R*-estimation method (Duchnowski 2010, 2013) and the M_{split} estimation method (Wiśniewski 2009, 2010; Duchnowski and Wiśniewski 2012; Zienkiewicz 2015). *R*-estimation, which is based on the application of a statistical rank test (Huber 1981; Feltovich 2003), has some interesting geodetic applications, such as elimination of systematic errors from an observation set (Duchnowski 2008b). *R*-estimation can also be considered as an estimation of differences between parameters of two functional models. Such differences can be considered as displacements of network points (Duchnowski 2008a, b, 2010, 2013). Duchnowski (2008a) demonstrated how to monitor the stability of the netpoints based on *R*-estimation principle. Duchnowski (2010) presented the application of the median absolute deviation (MAD) and average distance to the median (ADM) as a good support for *R*-estimates in the identification of unstable reference points. *M*-estimation, as a generalization of the maximum likelihood estimation, can be applied to particular geodetic applications. The M_{split} estimation can be expanded on q competitive functional models referring to the same observation set, indicated as $M_{\text{split}(q)}$. The differences between $M_{\text{split}(q)}$ estimates can be considered as assessments of point displacements in the network (Wiśniewski 2010). Duchnowski and Wiśniewski (2012) presented a method to estimate a shift between parameters of a functional model, which can also be applied when the functional models are not of full column rank. Duchnowski and Wiśniewski (2014) compared the two unconventional robust methods of the M_{split} estimation (shift-M_{split} estimate) and *R*-estimation. Zienkiewicz (2015) investigated the efficiency of the M_{split} estimation to determine the displacements of control points in an unstable reference system.

In both commonly used methods (i.e., IWST and global congruency testing), the LS adjustment is individually applied to the observations of each epoch. A drawback is that they are not optimal in the sense that they do not use the observations of both epochs simultaneously. In this contribution, the authors propose a new method that uses the observations of two epochs simultaneously and applies statistical tests. For the sake of brevity, this approach is hereafter called the *simultaneous adjustment of two epochs* (SATE) method. This method is applicable to one-dimensional (1D), two-dimensional (2D), or three-dimensional (3D) deformation networks with different types of observations, including distances, angles, global positioning system (GPS) baselines, and height difference.

The idea behind SATE originates from the works of Baarda (1968), Teunissen (2000), and Teunissen et al. (2005), in which some misspecifications were detected in the functional model using the statistical tests. Any issue that has not been modeled in the structure of the functional model is referred to as a *misspecification*, which could be due to the presence of blunders (Baarda 1968; Teunissen 2000), undetected pure and modulated frequencies in different geodetic time series (Amiri-Simkooei 2007, 2013; Amiri-Simkooei and Asgari 2012; Amiri-Simkooei et al. 2007, 2014), and displacement due to unstable netpoints in a geodetic network (present contribution).

The authors applied this idea to identify (un)stable points of a deformation-monitoring network. To identify the stable points, two hypotheses testing two functional models were put forward. In the null hypothesis, it was assumed that the point is stable, whereas in the alternative hypothesis, it was unstable. Therefore, the LS adjustment was performed on these two models and the results were compared using a statistical test, which is referred to as the generalized likelihood ratio (GLR) test. The GLR test allows one to decide between the original model under the null hypothesis and the extended model under the alternative hypothesis (Teunissen 2000).

There are methods based on the observation differences between the two epochs (Vaníček and Krakiwsky 1986; Nowel and Kamiński 2014), which also use the observations of both epochs simultaneously. However, there are a few differences with SATE. First, SATE is completely different from the method based on the observation differences because the underlying theoretical principles of the two methods are totally different. Second, there is no need to take the same observables for both epochs in the case of SATE—a requirement for the method based on the observation differences. Third, Nowel and Kamiński (2014) have proposed their robust estimation method based on the classical IWST method; it is only an improved variant of IWST. Furthermore, the method based on the observation differences has a number of limitations. First. the same observation structure in both epochs is required in this

method. The same geometric elements are then to be measured in both epochs. However, this is sometimes suboptimal, because a possible outlying observation, detected in one of the two epochs, is to be excluded from the other epoch. Second, the idea behind SATE allows one to use observations from more than two epochs, which is difficult to formulate for the method based on the observation differences.

This paper is organized as follows. The following section provides a brief review of two classical methods of detecting (un)stable points in a deformation network: the global congruency testing method and the IWST method. In a later section, a new method is presented to identify the stable points—namely, the SATE, method in which the observations of two epochs are simultaneously used in the least squares adjustment. An illustrative example relevant to the implementation of the proposed method is also presented. A subsequent section includes some simulation case studies on displacement-monitoring networks with different scenarios to investigate the efficacy of the proposed method on the identification of the unstable points. The results of a real landslide network are also provided in this section. Finally, some conclusions are made in the last section.

Point Stability Identification

Assume the observations of a deformation network have been measured over two different epochs denoted by t_1 and t_2. Each epoch is separately adjusted as an individual network. Therefore, for the two epochs ($i = 1, 2$), two sets of the unknown parameter vectors ($\hat{\mathbf{x}}_1, \hat{\mathbf{x}}_2$) along with their corresponding cofactor matrices ($\mathbf{Q}_{\hat{\mathbf{x}}_1}, \mathbf{Q}_{\hat{\mathbf{x}}_2}$), and the posterior variance factors ($\hat{\sigma}_{01}^2, \hat{\sigma}_{02}^2$) are estimated. The redundancy (degree of freedom) of the two networks are df_1 and df_2.

The first step of the deformation analysis is to check the compatibility of the estimated posterior variance factors of both epochs. To this end, the following two hypotheses are put forward (Setan 1995; Caspary 1987; Chen et al. 1990; Cooper 1987):

$$H_0 : \hat{\sigma}_{01}^2 = \hat{\sigma}_{02}^2 \qquad \text{versus} \qquad H_a : \hat{\sigma}_{01}^2 \neq \hat{\sigma}_{02}^2 \tag{1}$$

The test statistic is then of the form

$$\underline{T} = \frac{\underline{\hat{\sigma}}_{01}^2}{\underline{\hat{\sigma}}_{02}^2} \sim F_{\mathrm{df}_1,\mathrm{df}_2} \tag{2}$$

where an underscore indicates that a quantity is a random variable; and F = Fisher's distribution. With the significance level (α), the null hypothesis is accepted if $T < F_{\alpha;\mathrm{df}_1,\mathrm{df}_2}$ (generally $\alpha = 0.05$). If the test is rejected due to incompatible weighting between the two epochs or incorrect observable weighting scheme, any further analysis might be stopped.

After accepting the test on the posterior variance factors of two epochs [Eq. (2)], the $n \times 1$ displacement vector, with n being the dimension of the unknown vector, is defined as

$$\hat{\mathbf{d}} = \hat{\mathbf{x}}_2 - \hat{\mathbf{x}}_1 \tag{3}$$

with the cofactor matrix

$$\mathbf{Q}_{\hat{\mathbf{d}}} = \mathbf{Q}_{\hat{\mathbf{x}}_2} + \mathbf{Q}_{\hat{\mathbf{x}}_1} \tag{4}$$

assuming that $\hat{\mathbf{x}}_1$ and $\hat{\mathbf{x}}_2$ are uncorrelated.

Two commonly used methods used to identify the (un)stable points of a deformation-monitoring network are the congruency testing method and the IWST method.

Global Congruency Test

Global congruency testing is widely used to identify the stable points of a deformation-monitoring network. This method has been developed by Niemeier (1979) and van Mierlo (1978). Implementation of this method was later described by Fraser and Gruendig (1984). The method will iteratively remove one datum point at a time until the congruency test passes. More explanations on the global congruency test can also be found in Cooper (1987). The global congruency testing can be applied to identify whether or not the points of the network have remained stable during the time span of the two epochs. Based on the statistical tests, this method identifies the most possible group of points for which the value of the displacement test statistic does not exceed the critical value. In the deformation analysis using the congruency testing method, it is important that the displacement vector ($\mathbf{d}$) and its cofactor matrix ($\mathbf{Q_d}$) refer to a stable datum. For this purpose, the S-transformation is applied to transform the vector $\mathbf{d}$ and the matrix $\mathbf{Q_d}$ into a common datum as follows (see Baarda 1981; Teunissen 1985):

$$\mathbf{d}_1 = \mathbf{S}\mathbf{d} \quad \text{and} \quad \mathbf{Q}_{\mathbf{d}_1} = \mathbf{S}\mathbf{Q}_{\mathbf{d}}\mathbf{S}^{\mathbf{T}} \tag{5}$$

where

$$\mathbf{S} = \mathbf{I} - \mathbf{H}^{\mathbf{T}}(\mathbf{D}\mathbf{H}^{\mathbf{T}})^{-1}\mathbf{D} \tag{6}$$

where $\mathbf{d}_1$ and $\mathbf{Q}_{\mathbf{d}_1}$ = displacement vector and its cofactor matrix in the new datum, respectively; $\mathbf{I}$ = identity matrix; $\mathbf{H}$ = inner constraints datum matrix, which spans the null space of the design matrix; and $\mathbf{D}$ = datum matrix.

To investigate the stability of the selected datum points during the time span of two epochs, the following two hypotheses are put forward:

$$H_0 : E(\underline{\hat{\mathbf{d}}}) = E(\underline{\hat{\mathbf{x}}}_2) - E(\underline{\hat{\mathbf{x}}}_1) = 0 \tag{7}$$

indicating that there is no significance deformation for the selected datum point (i.e., no deformation exists). The alternative hypothesis is

$$H_a : E(\underline{\hat{\mathbf{d}}}) = E(\underline{\hat{\mathbf{x}}}_2) - E(\underline{\hat{\mathbf{x}}}_1) = \Delta \neq 0 \tag{8}$$

indicating that a group of selected datum points has not remained stable in the time span of the two epochs. In Eqs. (7) and (8), E stands for the expectation operator, and Δ is the $u \times 1$ expected displacement vector. The test statistic, known as the global congruency test, is set as follows:

$$\underline{\omega} = \frac{\Omega}{h\underline{\hat{\sigma}}_0^2} \sim F_{h,\mathrm{df}} \tag{9}$$

which has the central Fisher distribution with parameters h = rank of $\mathbf{Q}_{\hat{\mathbf{d}}}$ and df, under the null hypothesis. In Eq. (9), one has

$$\Omega = \underline{\hat{\mathbf{d}}}^{\mathbf{T}}\mathbf{Q}_{\hat{\mathbf{d}}}^{+}\underline{\hat{\mathbf{d}}} \tag{10}$$

where $\mathbf{Q}_{\hat{\mathbf{d}}}^{+}$ = Moore–Penrose inverse of the cofactor matrix ($\mathbf{Q}_{\hat{\mathbf{d}}}$). Also

$$\underline{\hat{\sigma}}_0^2 = \frac{\left(\mathrm{df}_1 \underline{\hat{\sigma}}_{01}^2 + \mathrm{df}_2 \underline{\hat{\sigma}}_{02}^2\right)}{\mathrm{df}} \tag{11}$$

is the total estimated variance factor in which $\mathrm{df} = \mathrm{df}_1 + \mathrm{df}_2$ is the total degrees of freedom.

If the test statistic exceeds the critical value of the F distribution, the null hypothesis is rejected at a significant level (α) (i.e., $\omega > F_{\alpha;h,\mathrm{df}}$). This indicates that some parts of the network do not remain stable in the time span of the two epochs (i.e., deformation has occurred). To identify which points are unstable, the contribution of each point to the quadratic form (Ω) in Eq. (10) should be obtained as $\Omega_j = \mathbf{d}_\mathbf{j}^{\prime\mathrm{T}} \mathbf{P}_\mathbf{j} \mathbf{d}_\mathbf{j}^{\prime}$ for each point in turn, where $\mathbf{d}_\mathbf{j}^{\prime} = \mathbf{P}_\mathbf{j}^{-1} \mathbf{P}_\mathbf{rj} \mathbf{d}_\mathbf{r} + \mathbf{d}_\mathbf{j}$, in which

$$\mathbf{d} = \begin{bmatrix} \mathbf{d_r} \\ \mathbf{d_j} \end{bmatrix} \text{ and } \mathbf{Q}_\mathbf{d}^{+} = \begin{bmatrix} \mathbf{P_r} & \mathbf{P_{rj}} \\ \mathbf{P_{jr}} & \mathbf{P_j} \end{bmatrix} \tag{12}$$

where the index $\mathbf{j}$ = deformed point; and the index $\mathbf{r}$ = other points.

The point that gives the maximum Ω_j is then identified as the unstable point and is to be excluded from the datum definition for further localization. To test whether the remaining points are deformed or not, the jth point can be excluded from the datum definition by an S-transformation on both $\mathbf{d}$ and $\mathbf{Q_d}$. The retained datum points are then tested for stability by congruency testing as follows [similar to Eq. (9)]:

$$\frac{\underline{\mathrm{d}}_\mathbf{r}^{\mathrm{T}} \mathbf{P}_\mathbf{r} \underline{\mathrm{d}}_\mathbf{r}}{(h-3k)\underline{\hat{\sigma}}_0^2} \sim F_{h-3k,\mathrm{df}} \tag{13}$$

where k = number of points already excluded from the datum definition; and $\mathbf{P_r} = (n-3k) \times (n-3k)$ submatrix of $\mathbf{Q}_\mathbf{d}^{+}$ according to Eq. (12). If the null hypothesis of the aforementioned statistical test is rejected [i.e., $\{(\mathbf{d}_\mathbf{r}^{\mathrm{T}} \mathbf{P_r} \mathbf{d_r})/[(h-3k)\hat{\sigma}_0^2]\} > F_{\alpha;h-3k,\mathrm{df}}$), the same localization procedure is repeated until the congruency test passes. As a result of the localization, unstable points are identified.

IWST

Another method to detect the (un)stable points of a network is based on the minimization of the L1 norm of the displacement vector (Chen 1983). This robust method is known as an IWST in geodetic literature. The method can easily be implemented through an iterative weighting scheme until the condition $\|\mathbf{d}\|_{L_1} = \sum_{i=1}^{n} |\mathbf{d}(i)| \rightarrow \min$ is met. Having the displacement vector and its cofactor matrix available, the stability of each point is checked through a single point test as

$$\underline{T}_j = \frac{\left(\hat{\mathbf{d}}_j^{(i)}\right)^{\mathbf{T}} \left(\mathbf{Q}_{\hat{\mathbf{d}}_j}^{(i)}\right)^{-1} \underline{\hat{\mathbf{d}}}_j^{(i)}}{c\underline{\hat{\sigma}}_0^2} \sim F_{c,df};\ j = 1, \ldots, n \tag{14}$$

where c = dimension of the network; and $\hat{\mathbf{d}}_s^{(i)}(j)$ = jth entry of the displacement vector after the ith iteration.

If the aforementioned test passes (i.e., $T_j < F_{\alpha;c,\mathrm{df}}$), the point is assumed to be stable at a significant level α; otherwise, it is unstable in the time span of two epochs. For more information about the IWST method, one may refer to Chen (1983) and Chen et al. (1990).

SATE

In both of the aforementioned methods, individual LS adjustment is carried out for each epoch of observations. These methods are not optimal because they do not use the observations of the two epochs simultaneously. A new method is proposed, the SATE method, which uses the observations of the two epochs simultaneously in the LS adjustment. The idea behind the proposed method originates from the works of Baarda (1968), Teunissen (2000), and Teunissen et al. (2005), in which some misspecifications in the functional model were detected using statistical tests. The same principle has already been applied by Amiri-Simkooei et al. (2007) concerning model identification of the GPS coordinate time series.

In the proposed method, to identify the (un)stable points of a deformation network, two hypotheses on the functional models are put forward. In the null hypothesis, it is assumed that all points of the monitoring network are stable during the time span of two epochs (i.e., no deformation has taken place). In the alternative hypothesis, however, it is assumed that one point is subject to movement in this time span. In other words, this (unstable) point has two series of coordinates in the first and second epochs. These two functional models are defined as

$$\text{Model 1}: \quad E(\underline{\mathbf{y}}) = \mathbf{Ax} \tag{15}$$

versus

$$\text{Model 2}: \quad E(\underline{\mathbf{y}}) = [\mathbf{A} \quad \mathbf{B}] \begin{bmatrix} \mathbf{x} \\ \boldsymbol{\zeta} \end{bmatrix} = \mathbf{Ax} + B\zeta \tag{16}$$

where $\underline{\mathbf{y}}$ = m-dimensional random vector of observations; $\mathbf{x}$ = n-vector of the unknown parameters; $\mathbf{A}$ = design matrix; $\boldsymbol{\zeta}$ = difference between the coordinates of the selected point from Epoch 1 to Epoch 2 (i.e., displacement of the point); and $\mathbf{B}$ = corresponding design matrix.

Model 1, presented in Eq. (15), is considered the basis or nominal model. The basic model can also include some disturbances or anomalies expressed by the matrix $\mathbf{B}$ and the vector $\boldsymbol{\zeta}$ in Model 2. They are caused by the instability of the points that invalidate the basis model. In the present approach, using statistical testing, one can check whether or not the observed data in both epochs *obey* the basis model in Eq. (15).

Assuming that the observations have the multivariate normal distribution, the following null and alternative hypotheses on the expectation of $\underline{\mathbf{y}}$ are put forward:

$$H_0 : E(\underline{\mathbf{y}}) \sim N_m(\mathbf{Ax}, \mathbf{C_y}) \tag{17}$$

versus

$$H_a : E(\underline{\mathbf{y}}) \sim N_m(\mathbf{Ax} + B\zeta, \mathbf{C_y}) \tag{18}$$

where N_m = m-dimensional normal distribution; and $\mathbf{C_y}$ = covariance matrix of the observables. The two hypotheses differ only in the specification of the functional model. The stochastic characteristics of both models are assumed to be identical. It is first assumed that the stochastic model is completely known (i.e., the covariance matrix $\mathbf{C_y}$ is known). This is the so-called σ *known* in the literature. It is then assumed that the covariance matrix is known up to the variance factor of the unit weight (σ_0^2) (i.e., $\mathbf{C_y} = \sigma_0^2 \mathbf{Q}$, where $\mathbf{Q}$ is the known cofactor matrix, but σ_0^2 is unknown to be estimated). This is referred to as σ *unknown*.

σ Known

To test the composite hypothesis (H_0) versus the composite hypothesis (H_a), the GLR test can be applied (see Teunissen 2000). The probability density function (PDF) of the observable vector ($\underline{y}$),

denoted by $f_y(y|x)$, is a function of x. It is referred to as the likelihood function of y, which is to be maximized for x restricted to the set Φ_0 for the null hypothesis, and for the unrestricted case $x \in \Phi$. The GLR test, yielding a binary decision, is defined as

$$\text{reject } H_0 \text{ if } \frac{\max\limits_{\mathbf{x}\in\Phi_0} f_y(y|x)}{\max\limits_{\mathbf{x}\in\Phi} f_y(y|x)} < a \tag{19}$$

and accepted otherwise, with $a \in (0, 1)$. The numerator implies maximization of the likelihood within the subset $\Phi_0 \subset \Phi$ put forward by the null hypothesis (H_0). The denominator amounts to a maximization over the whole parameter space (Φ). When the first maximum is, to a certain extent (specified by a), smaller than the second, the null hypothesis (H_0) with values for x restricted to $x \in \Phi_0$ is considered not sufficiently likely, and hence rejected (Teunissen et al. 2005).

In this contribution, the GLR test provides a decision on whether or not the additional unknowns due to the instability of the netpoints between the two epochs are to be taken into account by the vector $\boldsymbol{\zeta}$. If the observables are normally distributed, the GLR test, with Eqs. (17) and (18), yields

$$\text{reject } H_0 \text{ if } \frac{\max\limits_{\mathbf{x}} N_m(\mathbf{Ax}, \mathbf{C_y})}{\max\limits_{\mathbf{x},\boldsymbol{\zeta}} N_m(\mathbf{Ax}+\mathbf{B}\boldsymbol{\zeta}, \mathbf{C_y})} < a \tag{20}$$

and accepted otherwise, with $a \in (0, 1)$. One can show that H_0 is rejected if (Teunissen 2000)

$$\hat{\mathbf{e}}_\mathbf{0}^\mathbf{T}\mathbf{C_y^{-1}}\hat{\mathbf{e}}_\mathbf{0} - \hat{\mathbf{e}}_\mathbf{a}^\mathbf{T}\mathbf{C_y^{-1}}\hat{\mathbf{e}}_\mathbf{a} > \ln\frac{1}{a^2} = k_a \tag{21}$$

where $\hat{\mathbf{e}}_0$ and $\hat{\mathbf{e}}_\mathbf{a}$ = LS residuals under the null and alternative hypotheses, respectively. The test statistic is then of the form

$$\underline{T}_q = \underline{\hat{\mathbf{e}}}_0^\mathbf{T}\mathbf{C_y^{-1}}\underline{\hat{\mathbf{e}}}_0 - \underline{\hat{\mathbf{e}}}_\mathbf{a}^\mathbf{T}\mathbf{C_y^{-1}}\underline{\hat{\mathbf{e}}}_\mathbf{a} \tag{22}$$

where the index q = additional unknowns in the alternative hypothesis (i.e., the dimension of the vector $\boldsymbol{\zeta}$; $q = 3$ for 3D networks, $q = 2$ for 2D networks, and $q = 1$ for 1D networks). The test statistic in Eq. (22) is chi-square distributed as (Teunissen et al. 2005)

$$H_0 : \underline{T}_q \sim \chi^2(q, 0) \quad \text{versus} \quad H_a : \underline{T}_q \sim \chi^2(q, \lambda) \tag{23}$$

where the noncentrality parameter (λ) is given as

$$\lambda = \boldsymbol{\zeta}^\mathbf{T}\mathbf{B}^\mathbf{T}\mathbf{P}_\mathbf{A}^{\perp\mathbf{T}}\mathbf{C_y^{-1}}\mathbf{P}_\mathbf{A}^\perp B\zeta = \|\mathbf{P}_\mathbf{A}^\perp B\zeta\|_{\mathbf{C_y^{-1}}} \tag{24}$$

where $\mathbf{P}_\mathbf{A}^\perp = \mathbf{I}_m - A(\mathbf{A}^\mathbf{T}\mathbf{C_y^{-1}}\mathbf{A})^{-1}\mathbf{A}^\mathbf{T}\mathbf{C_y^{-1}}$ = orthogonal projector.

To determine whether or not the netpoints are stable, the GLR test is used to decide between the basis model under the null hypothesis and the extended model under the alternative hypothesis [i.e., $H_0 : \underline{T}_q \sim \chi^2(q, 0)$ versus $H_a : \underline{T}_q \sim \chi^2(q, \lambda)$]. Rejection of the null hypothesis (H_0) is interpreted as the instability of the points of the network during the two epochs.

σ Unknown

So far, the GLR test on the two hypotheses dealt with the case in which the covariance matrix ($\mathbf{C_y}$) of the observables is completely known. One can now also address the case in which the covariance matrix of the observables is decomposed into a known cofactor matrix ($\mathbf{Q}$) and an unknown variance factor of the unit weight (σ_0^2) (i.e., $\mathbf{C_y} = \sigma_0^2\mathbf{Q}$). This structure of the covariance matrix occurs in many practical applications.

Here, again, the same hypotheses (on the functional model) are formulated and tested as those in Eqs. (15) and (16), but now with the variance of unit weight (σ_0^2) as an (additional) unknown parameter. In the case of σ unknown, the test statistic for testing H_0 in Eq. (15) against H_a in Eq. (16) is of the form (Teunissen et al. 2005)

$$\underline{T}_q = \frac{1}{q\underline{\hat{\sigma}}_a^2}\underline{\hat{\zeta}}^\mathbf{T}\mathbf{B}^\mathbf{T}\mathbf{Q}^{-1}\mathbf{Q}_{\hat{\mathbf{e}}_0}\mathbf{Q}^{-1}B\underline{\hat{\zeta}} \tag{25}$$

where $\mathbf{Q}_{\hat{\mathbf{e}}_0}$ = cofactor matrix of the LS residuals under the null hypothesis; and $\underline{\hat{\sigma}}_a^2$ = unbiased estimator of the variance factor under the alternative hypothesis (H_a), given as

$$\underline{\hat{\sigma}}_a^2 = \frac{\underline{\hat{\mathbf{e}}}_\mathbf{a}^\mathbf{T}\mathbf{Q}^{-1}\underline{\hat{\mathbf{e}}}_\mathbf{a}}{m-n-q} \tag{26}$$

The test statistic of Eq. (25) is distributed as (Teunissen et al. 2005)

$$H_0 : \underline{T}_q \sim F(q, m-n-q, 0) \text{ versus } H_a : \underline{T}_q \sim F(q, m-n-q, \lambda) \tag{27}$$

with

$$\lambda = \frac{1}{\sigma^2}\boldsymbol{\zeta}^\mathbf{T}\mathbf{B}^\mathbf{T}\mathbf{Q}^{-1}\mathbf{Q}_{\hat{\mathbf{e}}_0}\mathbf{Q}^{-1}B\zeta \tag{28}$$

as the noncentrality parameter. A detailed explanation on the aforementioned derivations can be found in Teunissen et al. (2005).

A final practical comment on the representation of Eqs. (17) and (18) is in order. An equivalent representation to these equations is

$$\text{Model 1}: \quad E(\underline{\mathbf{y}}) = \mathbf{Ax} \tag{29}$$

versus

$$\text{Model 2}: \quad E(\underline{\mathbf{y}}) = [\mathbf{A}' \quad \mathbf{B}]\begin{bmatrix}\mathbf{x}\\ \boldsymbol{\zeta}'\end{bmatrix} = \mathbf{A}'\mathbf{x} + \mathbf{B}\boldsymbol{\zeta}' \tag{30}$$

where $\mathbf{A}'$ = new design matrix differing from the design matrix ($\mathbf{A}$) of Eqs. (29) and (16); and $\boldsymbol{\zeta}'$ = new coordinates of the selected point at Epoch 2 (and not the displacement from Epoch 1 to Epoch 2). The matrix $\mathbf{B}$ is identical to the one given in Eq. (16). In both representations, either Eqs. (15) and (16) or Eqs. (29) and (30), the test statistic can be obtained through Eqs. (22) and (25) in the cases of σ known or σ unknown, respectively. Using an example, how the matrices of the proposed method in both representations can be formed is now illustrated.

Illustrative Example

Using a simple example, the authors now describe how to use the proposed method in practice. A leveling network consisting of four points and six leveling lines is used (Fig. 1). The network can be regarded as a control network located outside the deformable part of the body, or the object being monitored. Therefore, the object points can be placed inside the network.

The aim is to test whether or not the network's points have any significant vertical deformation. For this purpose, the network was observed over two different epochs. The height differences

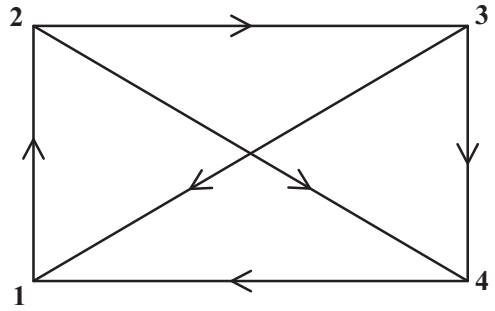

Fig. 1. Leveling network of illustrative example

measured at the first and the second epoch are $\mathbf{y}_1 = [\Delta H_{12}, \Delta H_{23}, \Delta H_{34}, \Delta H_{41}, \Delta H_{31}, \Delta H_{24}]^T$ and

$$\mathbf{y}_2 = [\Delta H_{31}, \Delta H_{12}, \Delta H_{34}, \Delta H_{24}, \Delta H_{23}, \Delta H_{41}]^T$$

where ΔH_{ij} stands for $H_j - H_i$ (i.e., the height difference measured between points i and j of the leveling network). Based on the observations, the design matrices for the two epochs are of the form

$$\mathbf{A}_1 = \begin{bmatrix} -1 & 1 & 0 & 0 \\ 0 & -1 & 1 & 0 \\ 0 & 0 & -1 & 1 \\ 1 & 0 & 0 & -1 \\ 1 & 0 & -1 & 0 \\ 0 & -1 & 0 & 1 \end{bmatrix} \tag{31}$$

for Epoch 1, and

$$\mathbf{A}_2 = \begin{bmatrix} 1 & 0 & -1 & 0 \\ -1 & 1 & 0 & 0 \\ 0 & 0 & -1 & 1 \\ 0 & -1 & 0 & 1 \\ 0 & -1 & 1 & 0 \\ 1 & 0 & 0 & -1 \end{bmatrix} \tag{32}$$

for Epoch 2. The final design matrix ($\mathbf{A}$) and the observations vector (y), given in Eqs. (15) and (16), can then be obtained by

$$\mathbf{A} = \begin{bmatrix} \mathbf{A}_1 \\ \mathbf{A}_2 \end{bmatrix}_{12\times 4} \text{ and } \underline{\mathbf{y}} = \begin{bmatrix} \underline{\mathbf{y}}_1 \\ \underline{\mathbf{y}}_2 \end{bmatrix}_{12\times 1} \tag{33}$$

The basic model, assuming that all network points are stable during the time span of the two epochs, is the same as that in Eq. (15), in which the unknown vector is the heights of the four points, $\mathbf{x} = [H_1 \quad H_2 \quad H_3 \quad H_4]^T$. This is what one deals with in the null hypothesis.

Now the point stability during the time periods of the two epochs is checked. Based on the proposed method, each point must be tested separately. Here, one starts with Point 1. To check the stability of this point, it is assumed that this point has a significant vertical deformation. This indicates that Point 1 has a new height in the second epoch, which differs from its height in the first epoch. Therefore, two different heights must be assumed for Point 1 in this case. Model 2 [Eq. (16)] is then of the form

$$E(\underline{\mathbf{y}}) = [\mathbf{A} \quad \mathbf{B}] \begin{bmatrix} \mathbf{x} \\ \boldsymbol{\zeta} \end{bmatrix} = \mathbf{A}\mathbf{x} + \mathbf{B}\boldsymbol{\zeta} \tag{34}$$

where the additional unknown parameter (ζ) is defined to express the vertical deformation of Point 1 (i.e., $\zeta = H_1' - H_1$, where H_1 and H_1' are the heights of Point 1 at the first and second epoch, respectively). The unknown vector (x) is identical to that in Model 1 (i.e., $\mathbf{x} = [H_1 \quad H_2 \quad H_3 \quad H_4]^T$). In Eq. (34), matrix $\mathbf{B}$ reads

$$\mathbf{B} = [0 \quad 0 \quad 0 \quad 0 \quad 0 \quad 0 \quad 1 \quad -1 \quad 0 \quad 0 \quad 0 \quad 1]^T \tag{35}$$

Furthermore, one can use the alternative model given in Eq. (30) as follows:

$$E(\underline{\mathbf{y}}) = [\mathbf{A}' \quad \mathbf{B}] \begin{bmatrix} \mathbf{x} \\ \boldsymbol{\zeta}' \end{bmatrix} = \mathbf{A}'\mathbf{x} + \mathbf{B}\boldsymbol{\zeta}' \tag{36}$$

where the additional unknown parameter (ζ') stands for the new height of Point 1 at Epoch 2 (i.e., $\zeta' = H_1'$, in which H_1' is the height of Point 1 at the second epoch). The unknown vector (x) is also identical to the previous case (i.e., $\mathbf{x} = [H_1 \quad H_2 \quad H_3 \quad H_4]^T$). In Eq. (36), the matrix $[\mathbf{A}' \quad \mathbf{B}]$ can be given as follows:

$$[\mathbf{A}' \quad \mathbf{B}] = \left[\begin{array}{cccc:c} \overbrace{-1 & 1 & 0 & 0}^{\mathbf{A}'} & \vdots & \overbrace{0}^{\mathbf{B}} \\ 0 & -1 & 1 & 0 & \vdots & 0 \\ 0 & 0 & -1 & 1 & \vdots & 0 \\ 1 & 0 & 0 & -1 & \vdots & 0 \\ 1 & 0 & -1 & 0 & \vdots & 0 \\ 0 & -1 & 0 & 1 & \vdots & 0 \\ 0 & 0 & -1 & 0 & \vdots & 1 \\ 0 & 1 & 0 & 0 & \vdots & -1 \\ 0 & 0 & -1 & 1 & \vdots & 0 \\ 0 & -1 & 0 & 1 & \vdots & 0 \\ 0 & -1 & 1 & 0 & \vdots & 0 \\ 0 & 0 & 0 & -1 & \vdots & 1 \end{array}\right] \tag{37}$$

Obviously, the design matrix $\mathbf{A}'$ in Eq. (37) differs from the design matrix $\mathbf{A}$ in Eq. (34). However, it is noted that $R([\mathbf{A} \quad \mathbf{B}]) = R([\mathbf{A}' \quad \mathbf{B}])$, where R is the range space of a matrix. This in fact verifies the equivalence of these two formulations from a theoretical point of view.

The first computational step is to apply the LS adjustment to both of the functional models [i.e., to the basic and extended models given in either Eqs. (15) and (16) or Eqs. (29) and (30)]. The same strategy is now repeated for the other points (e.g., Points 2, 3, and 4). The test statistics given in Eq. (22) or (25) are then computed for these points (in total, four values for this example). The point with the largest value of the test statistic is then tested. The rejection of the null hypothesis indicates that this point (with the largest test statistic) has significant vertical deformation (i.e., the point is unstable). The functional model is then adopted by including the column (s) of the matrix $\mathbf{B}$ to the design matrix $\mathbf{A}$ (i.e., $\mathbf{A} \leftarrow [\mathbf{A}' \mathbf{B}]$). Accordingly, the unknown vector $\mathbf{x} = [H_1 \; H_2 \; H_3 \; H_4]^T$ is to be modified as $\mathbf{x} = [H_1 \quad H_2 \quad H_3 \quad H_4 \quad H_i']^T$, where $i = 1, 2, 3$, or 4. The same procedure is now applied to the remaining points to identify further possible unstable points. The procedure stops when the null hypothesis is not rejected. As a result, the (un)stable points of the network are identified. It is noted, in each step, that the matrix $\mathbf{B}$

has only one column for the leveling network. The columns then become 2 and 3 for the 2D and 3D networks, respectively.

Numerical Results and Discussions

To investigate the efficacy of the SATE method compared with the two classical methods, the global congruency testing method and the IWST method, the results of a real GPS deformation-monitoring network are provided. Furthermore, simulation studies are presented in this contribution.

Experiment Setup

In this section, the performance of the proposed method is evaluated using a real data set. The area under study is close to the Hardang village located in the southwest of Lenjan, Isfahan province, Iran (latitude: 32.27°; longitude: 51.19°). A GPS network consisting of 30 points was observed to monitor the deformation due to landslide. The network consists of an outer frame of four stations, indicated by the squares in Fig. 2. They surround the inner stations, indicated by the circles in the same figure. The deformation of the Hardang network was monitored using two GPS measurement campaigns. The first campaign was carried out from September 3rd to 16th, 2010. The second campaign was carried out from June 27th to 29th, 2011. The measurements were carried out with the dual-frequency GPS receivers of Leica System 1200 (Leica Geosystems AG, St. Gallen, Switzerland). The measurements were postprocessed with the Leica GeoOffice 5.0 software in the L1 + L2 frequency type. The elevation cutoff angle was set to 15°. The ambiguities were resolved and introduced into the observation equations accordingly. The adjustment network was performed. The baseline vectors presented in Tables 1 and 2 were then extracted as the processing output. The GPS baselines, observed in both epochs, are listed in Tables 1 and 2. The redundancy (degree of freedom) of the two networks is $df_1 = (8 \times 3) - (4 \times 3) + 3 = 15$ and $df_2 = (5 \times 3) - (4 \times 3) + 3 = 6$.

Unstable points were then detected using the three methods. Table 3 summarizes the results, which indicate that the three methods identified the same unstable points. This confirms that the proposed method works well. However, due to the small number of

Table 1. GPS Baseline Observed at Epoch 1 (September 3–16, 2010)

From	To	ΔX (m)	ΔY (m)	ΔZ (m)
BM1	BM2	9.3553	115.8320	–96.8290
BM1	BM2	9.3562	115.8333	–96.8281
BM1	BM3	113.5095	194.4388	–212.3491
BM1	BM3	113.5083	194.4370	–212.3505
BM1	BM4	191.2829	–22.3190	–141.6007
BM3	BM2	–104.1525	–78.6047	115.5216
BM4	BM2	–181.9274	138.1512	44.7715
BM4	BM3	–77.7714	216.7598	–70.7463

Table 2. GPS Baseline Observed at Epoch 2 (June 27–29, 2011)

From	To	ΔX (m)	ΔY (m)	ΔZ (m)
BM4	BM2	–181.9197	138.1613	44.7815
BM4	BM2	–181.9182	138.1594	44.7813
BM1	BM3	113.5116	194.4437	–212.3457
BM1	BM2	9.3597	115.8400	–96.8233
BM4	BM3	–77.7660	216.7649	–70.7400

Fig. 2. Hardang deformation-monitoring network shown in Google Earth (Image ©2016 DigitalGlobe, © 2016 Google)

stations used in this experiment, the superiority of the proposed method over the other two methods cannot be tested. Thus, simulated observations were used to reach this goal.

Table 3. Stable and Unstable Points of Hardang Deformation Monitoring Network Detected Using Three Different Methods

Method	Stable points	Unstable points
Global congruency test (Method I)	2, 3	1, 4
IWST (Method II)	2, 3	1, 4
SATE (Method III)	2, 3	1, 4

Table 4. Four Cases of Simulation Setup of a 3D GPS Deformation-Monitoring Network

Case	Network configuration	Observation pattern	Unstable points	Deformations
1	Fixed	Fixed	Fixed	Given
2	Fixed	Random	Fixed	Given
3	Fixed	Random	Random	Random
4	Random	Random	Random	Random

Simulation Setup

To better illustrate the performance of the proposed method over the other two methods, simulations were performed for four different scenarios of a 3D GPS deformation-monitoring network (Table 4). The simulated observations used in the four cases, provided in Table 4, are the GPS baselines between the network's points. For all hypotheses testing, the significance level is set to $\alpha = 0.05$.

Case 1

In this case, a simple network was used to assess the performance of the proposed method. This GPS network consists of 10 points (Fig. 3). The 3D coordinates of the GPS stations are presented in Table 5. The monitoring network consists of two epochs of observations. For the second epoch, the positions of four points (2, 3, 4, and 6) were changed by the values specified in Table 6. In this example, a specified (fixed) observation pattern is used in which all possible baselines, equal to the two-combinations of all of the network's points as C (10,2) = 45, were simulated. Fig. 3 also shows the selected observation schema.

The nominal precision of 5 mm for each of the GPS baselines is assumed. For the designed network in Fig. 3, the coordinate differences are computed from the coordinates of the points for each

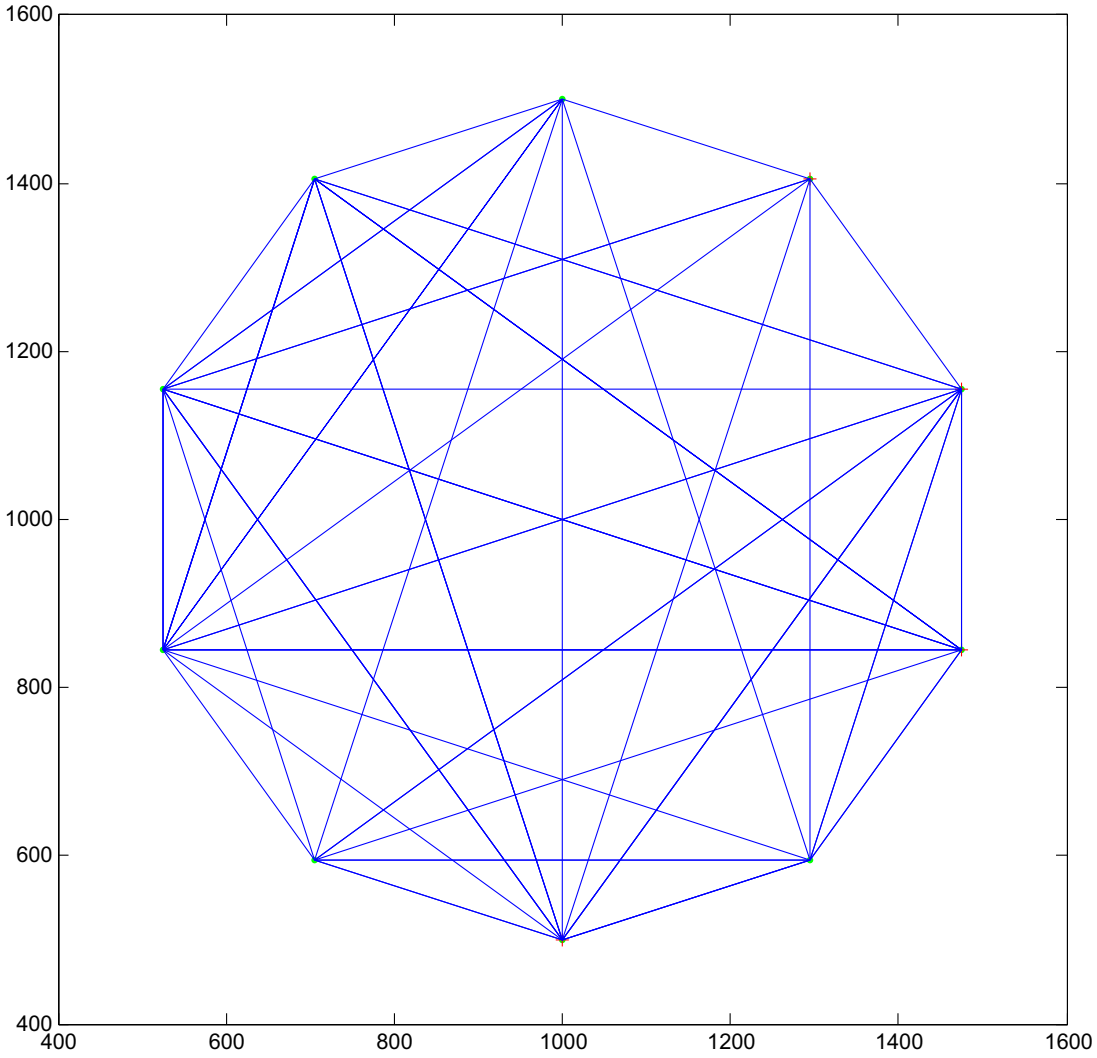

Fig. 3. Simulated GPS network for Case 1 (first epoch)

epoch, which are not yet affected by random errors; in fact, they are perfect observations. As a next step, all errorless observations are contaminated by white Gaussian noise with a mean of zero and a standard deviation of 5 mm. Therefore, two epochs of observations are generated for the simulated GPS network.

Network adjustment of each epoch was then carried out. Afterward, the a posteriori variance factors of both epochs, given in Eq. (2), were tested for their compatibility. If the test was rejected, this simulated network was excluded and another one was simulated. The simulation was repeated over 500 independent runs. For each run, the point stability analysis was followed by the two classical methods and the SATE method. For each run, the detected unstable points using the three different methods were compared with the actual unstable points introduced earlier in Table 6. The percentage of runs for which the detected unstable points are identical to those given in Table 6 is provided in Table 7 for the three methods.

The results indicate that the SATE method has better performance over the two classical methods of the global congruency testing and the IWST. This is mainly because the SATE method uses the observations of the two epochs simultaneously, whereas the other two methods use the individual LS adjustment of each epoch separately. The use of the simultaneous adjustment method is always advantageous because the observations are used in an optimal manner.

Table 5. 3D Coordinates of GPS Network Points for Case 1 (First Epoch)

Point number	ΔX (m)	ΔY (m)	ΔZ (m)
1	1,000.001	1,500.001	9.751
2	1,293.893	1,404.509	10.003
3	1,475.529	1,154.509	10.341
4	1,475.529	845.492	9.768
5	1,293.893	595.492	10.203
6	1,000.001	500.001	10.146
7	706.108	595.492	10.265
8	524.472	845.492	10.202
9	524.472	1,154.509	10.245
10	706.108	1,404.509	9.681

Table 6. Deformation Applied to Positions of Points 2, 3, 4, and 6 in Table 5 (for Second Epoch)

Point number	ΔX (m)	ΔY (m)	ΔZ (m)
2	0.006	–0.001	0.011
3	–0.002	–0.010	0.004
4	–0.010	–0.007	0.000
6	–0.004	0.006	–0.008

Table 7. Correct Detection of Unstable Points (Percentage) Using Three Different Methods for Cases 1 and 2

Case	Method I (%)	Method II (%)	Method III (%)
1	87.0	97.8	98.6
2	73.8	84.5	86.4

Case 2

In this case, the same network points as those given in Table 5 were used. The unstable points with their deformations were chosen from Table 6. However, one has a random observation pattern instead of the fixed observation schema in Fig. 3. Similar to the strategy explained in Case 1, the simulation procedure was repeated over 500 independent runs. In a similar manner, the percentage of the correct detection of the unstable points using the three different methods was computed and is listed in Table 7. For this case study, the results indicate that the performance of the proposed method on identification of unstable points is approximately 2 and 13% better than the IWST method and the global congruency testing method, respectively.

Case 3

The same network consisting of 10 points at the positions provided in Table 5 was now used. The number of unstable points as well as their corresponding deformations was randomly selected. The number of unstable points can randomly be selected between 1 and 8 for each run. The deformation vector of the selected unstable points was also randomly chosen within a sphere of radius R. The radius R was randomly selected in the interval of $[\mathrm{SF} \times \sigma_y, 2\mathrm{SF} \times \sigma_y]$, where SF is a scale factor and σ_y is the standard deviation of the observations (5 mm). Smaller SF values provide a smaller deformation sphere. The deformation vector ($\vec{\mathbf{d}}$), being added to the selected unstable point, is then obtained as

$$\vec{\mathbf{d}} = R[\ \cos V \cos Az \quad \cos V \sin AZ \quad \sin V\ ]^T \tag{38}$$

where Az and V = azimuthal and vertical angles, respectively; they are also randomly changed in the intervals of (0 to 360°) and

Table 8. Percentage of Correct Detection of Unstable Points and Incorrect Detection of Stable Points (Identified as Unstable) Corresponding to Case 3 Using Three Different Methods for SF = 1, 2, 3, and 9 (Total Number of Points Is 10,000)

SF	Method	Number of unstable points	Number of detected unstable points	Percentage of correct detection	Number of detected stable points as unstable points	Percentage of incorrect detection
1	I	3,647	1,574	43.1	183	2.9
	II		2,012	55.2	276	4.3
	III		2,190	60.0	361	5.7
2	I	3,575	2,997	83.8	122	1.9
	II		3,205	89.6	330	5.1
	III		3,310	92.6	339	5.3
3	I	3,564	3,377	94.7	121	1.9
	II		3,469	97.3	368	5.7
	III		3,500	98.2	356	5.5
9	I	3,628	3,627	99.9	61	0.96
	II		3,628	100.0	374	5.9
	III		3,628	100.0	303	4.7

(–90 to 90°). Here again, the simulation procedure was repeated over 1,000 independent runs (1,000 networks) for different values of SF (i.e., SF = 1, 2, 3, and 9). Table 8 outlines the percentage of the correct detection of the unstable points as well as the incorrect detection of stable points (identified as unstable) using the three methods. The total number of the points is equal to 10,000 (i.e., 10 netpoints for each of the 1,000 independent run).

A few observations from the results of this table can be highlighted. First, the proposed method (Method III) identifies the unstable points of the network more efficiently than the other two methods, for all values of SF. Second, the percentage of correct detection of the unstable points using the three different methods increases when SF increases. Third, the performance of the proposed method is obviously better than that of the other two methods when the deformation of the network is small (SF is small). Therefore, the choice of an appropriate method becomes important for a network with small deformations. The proposed method is thus considered to be appropriate for unstable point identification in small-deformation networks. A final remark on the results presented in this table is in order. The last column provides the percentage of the incorrect detection of stable points as unstable ones. On average, in 5.3% of the cases, the proposed method incorrectly identifies the stable points to be unstable. Although this is considered to be a disadvantage of the proposed method, leaving aside a stable point from the datum definition may not cause a serious problem; still, the datum can be defined on other stable points.

To better compare the performance of the three methods, the percentage of cases in which the methods work completely successfully over the 1,000 independent runs (i.e., the method succeeds if all unstable points are detected, and none of the stable points is identified as unstable) is provided in Table 9. The results indicate that the proposed method outperforms the other two methods.

Table 9. Percentage of Successful Detection over the 1,000 Independent Runs Corresponding to Case 3 Using Three Different Methods for SF = 1, 2, 3, and 9 (Total Number of Networks Is 1,000)

SF	Method	Number of successful detections	Percentage of successful detection
1	I	87	8.7
	II	222	22.2
	III	250	25.0
2	I	593	59.3
	II	761	76.1
	III	815	81.5
3	I	861	86.1
	II	941	94.1
	III	965	96.5
9	I	999	99.9
	II	1,000	100
	III	1,000	100

Case 4

In the last simulation scenario, a completely random network (i.e., random network configuration, random observation pattern, random unstable points with a random deformation) was considered. The number of netpoints can randomly be changed between 5 and 40 for each run. The horizontal position of the network points is also randomly selected within a square with a side length of 10 km. Their heights are randomly chosen in the interval of 0–100 m. The number of unstable points is randomly selected in the interval of 1 to $n-2$, in which n is the number of points. Also, the deformation of the selected unstable points is randomly selected. Here again, the deformation was selected as a function of SF in the interval of [SF $\times$ σ_y, 2SF $\times$ σ_y]. The simulation procedure was repeated over 1,000 independent runs for the different values of SF (i.e., SF = 1, 2, 3, and 9). In each run, the nominal precision of 1–5 mm was randomly selected for the observables. This error was then applied to the computed errorless observables described earlier.

After simulating a completely random network over 1,000 independent runs for different values of SF, one can obtain the percentage of the correct detection of the unstable points using the three methods described earlier (see Table 10). The proposed method performs the best compared to the IWST method and the global congruency testing method.

Similarly, the percentage of the cases in which the methods work completely successfully over the 1,000 independent runs (i.e., the method succeeds if all of the unstable points are detected, and none of the stable points is classified as unstable) is provided in Table 11. Again, the results indicate that the proposed method outperforms the other two methods, especially when the deformations are small.

Concluding Remarks

An important issue in the deformation- and displacement-monitoring networks is identification of the (un)stable points between

Table 10. Correct Detection of Unstable Points and Incorrect Detection of Stable Points as Unstable Points (Percentage) Corresponding to Case 4 Using Three Different Methods for SF = 1, 2, 3, and 9

SF	Method	Total Number of points	Number of unstable points	Number of detected points	Percentage of correct detection	Number of detected stable points as unstable points	Percentage of incorrect detection
1	I	21,934	7,807	2,424	31.0	1,199	8.5
	II			2,769	35.5	1,307	9.2
	III			3,299	42.3	1,539	10.9
2	I	21,824	7,861	5,631	71.6	1,143	8.2
	II			5,889	74.9	1,282	9.2
	III			6,426	81.7	1,472	10.5
3	I	22,105	8,022	7,022	87.5	1,015	7.2
	II			7,259	90.5	1,339	9.5
	III			7,600	94.7	1,466	10.4
9	I	22,338	8,275	8,260	99.8	726	5.2
	II			8,264	99.9	1,369	9.7
	III			8,273	99.9	1,459	10.3

Table 11. Percentage of Successful Detection over the 1,000 Independent Runs Corresponding to Case 4 Using Three Different Methods for SF = 1, 2, 3, and 9 (Total Number of Networks Is 1,000)

SF	Method	Number of successful detection	Percentage of successful detection
1	I	73	7.3
	II	115	11.5
	III	125	12.5
2	I	278	27.8
	II	417	41.7
	III	470	47.0
3	I	496	49.6
	II	670	67.0
	III	761	76.1
9	I	985	98.5
	II	992	99.2
	III	998	99.8

the measurement campaigns. There are already two methods in the geodetic literature that identify the unstable points of a network: the global congruency testing method and the IWST method, which minimizes the L1 norm of the displacement vector. In both methods, individual LS adjustment is applied to the observations of each epoch. However, they are not optimal in the sense that they do not adjust the observations of both epochs simultaneously. In this paper, a method was proposed that uses the observations of two epochs simultaneously in the LS adjustment. This method can be applied to 1D, 2D, or 3D networks with different types of observations, such as distances, angles, GPS baselines, and height differences. Two hypothesis tests, introduced into the functional model, were put forward. In the null hypothesis, the point was assumed to be stable, whereas in the alternative one, it was unstable. The LS adjustment was applied to these two models, and the results were compared using statistical tests. It could then be determined whether or not this point was stable in the time span of the two epochs.

To investigate the performance of the proposed method, the observations of a real GPS deformation-monitoring network were used. The results indicated that the three methods identified the same unstable points. Furthermore, a few simulation case studies were carried out. The simulated results on the deformation-monitoring networks with different scenarios showed that the proposed method always performs the best. This method can thus be introduced as a reliable method that provides superior results to the two existing classical methods.

References

Amiri-Simkooei, A. R. (2007). "Least-squares variance component estimation: Theory and GPS applications." Ph.D. thesis, Delft Univ. of Technology, Delft, The Netherlands.

Amiri-Simkooei, A. R. (2013). "On the nature of GPS draconitic year periodic pattern in multivariate position time series." *J. Geophys. Res. B: Solid Earth*, 118(5), 2500–2511.

Amiri-Simkooei, A. R., and Asgari, J. (2012). "Harmonic analysis of total electron contents time series: Methodology and results." *GPS Solutions.*, 16(1), 77–88.

Amiri-Simkooei, A. R., Tiberius, C. C. J. M., and Teunissen, P. J. G. (2007). "Assessment of noise in GPS coordinate time series: Methodology and results." *J. Geophys. Res.*, 112(B7), B07413.

Amiri-Simkooei, A. R., Zaminpardaz, S., and Sharifi, M. A. (2014). "Extracting tidal frequencies using multivariate harmonic analysis of sea level height time series." *J. Geodesy*, 88(10), 975–988.

Aydin, C. (2011). "On the power of global test in deformation analysis." *J. Surv. Div.*, 138(2), 51–56.

Baarda, W. (1968). "A testing procedure for use in geodetic networks." *Technical Rep., Publication on Geodesy*, Vol. 2(5), Netherlands Geodetic Commission, Delft, The Netherlands.

Baarda, W. (1981). *S-transformations and criterion matrices*, 2nd Ed., *Publications on Geodesy*, Rijkscommissie voor Geodesie, Delft, The Netherlands.

Caspary, W. F. (1987). *Concepts of network and deformation analysis*, 1st Ed., School of Surveying, Univ. of New South Wales, Monograph 11, Kensington, NSW, Australia.

Chen, Y. Q. (1983). "Analysis of deformation surveys–A generalized method." Ph.D. dissertation, Dept. of Geodesy and Geomatics Engineering, *Technical Rep. No. 94*, Univ. of New Brunswick, Fredericton, New Brunswick, Canada.

Chen, Y. Q., Chrzanowski, A., and Secord, J. M. (1990). "A strategy for the analysis of the stability of reference points in deformation surveys." *Can. Inst. Surv. Mapp. J.*, 44(2), 141–149.

Chrzanowski, A., Chen, Y. Q., and Secord, J. M. (1986). "Geometrical analysis of deformation surveys." *Proc., Deformation Measurements Workshop*, UNB Canadian Centre for Geodetic Engineering, Fredericton, NB, Canada, 170–206.

Cooper, M. A. (1987). *Control survey in civil engineering*, William Collins Sons & Co. Ltd., London.

Denli, H. H. (2008). "Stable point research on deformation networks." *Surv. Rev.*, 40(307), 74–82.

Duchnowski, R. (2008a). "Geodetic application of R-estimation: Leveling network examples." *Proc., 13th FIG Symp. on Deformation Measurement and Analysis and 4th Symp. on Geodesy for Geotechnical and Structural Engineering (CD-ROM)*, Laboratorio Nacional de Engenharia Civil, Lisbon, Portugal.

Duchnowski, R. (2008b). "R-estimation and its application to the LS adjustment." *Boll. Geod. Sci. Affini.*, 67(1), 21–30.

Duchnowski, R. (2010). "Median-based estimates and their application in controlling reference mark stability." *J. Surv. Div.*, 10.1061/(ASCE)SU.1943-5428.0000014, 47–52.

Duchnowski, R. (2013). "Hodges–Lehmann estimates in deformation analyses." *J. Geod.*, 87(10), 873–884.

Duchnowski, R., and Wiśniewski, Z. (2012). "Estimation of the shift between parameters of functional models of geodetic observations by applying M_{split} estimation." *J. Surv. Div.*, 10.1061/(ASCE)SU.1943-5428.0000062, 1–8.

Duchnowski, R., and Wiśniewski, Z. (2014). "Comparison of two unconventional methods of estimation applied to determine network point displacement." *Surv. Rev.*, 46(339), 401–405.

Erdogan, B., and Hekimoglu, S. (2014). "Effect of subnetwork configuration design on deformation analysis." *Surv. Rev.*, 46(335), 142–148.

Feltovich, N. (2003). "Nonparametric tests of differences in medians: Comparison of the Wilcoxon–Mann–Whitney and robust rank-order tests." *Exp. Econ.*, 6(3), 273–297.

Forward, T. A. (2002). "Quasi-continuous GPS steep slope monitoring: A multi-antenna array approach." Ph.D. thesis, Dept. of Spatial Sciences, Curtin Univ. of Technology, Perth, Western Australia.

Fraser, C., and Gruendig, L. (1984). "The analysis of photogrammetric deformation measurements on Turtle Mountain." *Engineering Surveys Conf.*, International Federation of Surveyors, Commission 6, Washington, DC.

Hekimoglu, S., Demirel, H., and Aydin, C. (2002). "Reliability of the conventional deformation analysis methods for vertical networks." *FIG XXII International Congress*, International Federation of Surveyors, Washington, DC.

Hekimoglu, S., and Erdogan, B. (2012). "New median approach to define configuration weakness of deformation networks." *J. Surv. Div.*, 10.1061/(ASCE)SU.1943-5428.0000080, 101–108.

Hekimoglu, S., Erdogan, B., and Butterworth, S. (2010). "Increasing the efficacy of the conventional deformation analysis methods: Alternative strategy." *J. Surv. Div.*, 10.1061/(ASCE)SU.1943-5428.0000018, 53–62.

Hekimoglu, S., and Koch, K. R. (1999). "How can reliability of robust methods be measured?" *Proc., 3rd Turkish-German Joint Geodetic*

Days, M. O. Altan, ed., Vol. 1, Istanbul Technical University, Istanbul, Turkey, 1179–196.
Hekimoglu, S., and Koch, K. R. (2000). "How can reliability of the test for outliers be measured?" *Allg. Vermes. Nachr.*, 107, 247–252.
Huber, P. J. (1981). *Robust statistics*, Wiley, New York.
Niemeier, W. (1979). "*Zur Kongruenz mehrfach beobachteter geodätischer Netze*." Universität Hannover, Hannover, Germany.
Niemeier, W. (1985). *Anlage von Überwachungsnetzen. Geodaetische netze in landes-und ingenieurvermessung II*, H. Pelzer, ed., Verlag Konrad Wittwer, Stuttgart, Germany, 527–558 (in German).
Nowel, K., and Kamiński, W. (2014). "Robust estimation of deformation from observation differences for free control networks." *J. Geod.*, 88(8), 749–764.
Rüeger, J. M. (2006). "Overview of geodetic deformation measurements of dam." *Annual Congress of the Australian National Committee on Large Dams (ANCOLD)*, 20–22 November, Sydney, Australia.
Setan, H. (1995). "Functional and stochastic models for geometrical detection of spatial deformation in engineering: A practical approach." Ph.D. thesis, Dept. of Civil Engineering, City Univ., London.
Setan, H., and Sing, R. (2001). "Deformation analysis of a geodetic monitoring network." *Geomatica*, 55(3), 333–346.
Setan, H., Som, Z. A. M., and Idris, K. M. (2003). "Deformation detection of lightweight concrete block using geodetic and non-geodetic methods." *11th FIG Symp. on Deformation Measurements*, Stathis Stiros, ed., University of Patras, Patras, Greece.
Taşçi, L. (2010). "Analysis of dam deformation measurements with the robust and non-robust methods." *Sci. Res. Essays*, 5(14), 1770–1779.
Teunissen, P. J. G. (1985). "Zero order design: Generalized inverses, adjustments, the datum problem and S-transformations." *Optimization and design of geodetic networks*, E. W. Grafarend and F. Sanso, eds., Springer, New York, 11–55.
Teunissen, P. J. G. (2000). "Testing theory an introduction." *Series on mathematical geodesy and positioning*, Delft Univ. Press ⟨http://www.vssd.nl⟩ (Dec. 15, 2010).
Teunissen, P. J. G., Simons, D. G., and Tiberius, C. C. (2005). *Probability and observation theory*, Delft Univ. of Technology, Delft, The Netherlands.
Vaníček, P., and Krakiwsky, E. J. (1986). *Geodesy: The concepts*, Elsevier, Amsterdam, The Netherlands.
van Mierlo, J. (1978). "A testing procedure for analysing geodetic deformation measurements." *Proc., 2nd Int. Symp. on Deformation Measurements by Geodetic Methods*, Wittwer, Stuttgart, Germany, 321–353.
Wiśniewski, Z. (2009). "Estimation of parameters in a split functional model of geodetic observations (Msplit estimation)." *J. Geod.*, 83(2), 105–120.
Wiśniewski, Z. (2010). "$M_{split(q)}$ estimation: Estimation of parameters in a multi split functional model of geodetic observations." *J. Geod.*, 84(6), 355–372.
Zienkiewicz, H. M. (2015). "Application of M_{split} estimation to determine control points displacements in networks with unstable reference system." *Surv. Rev.*, 47(342), 174–180.